Available online at www.sciencedirect.com

Catalysis Today 104 (2005) 200–204

www.elsevier.com/locate/cattod

Phenol cogeneration with electricity by using in situ generated H_2O_2 in a H_2–O_2 PEMFC reactor

Rui Cai [a], Shuqin Song [b], Baofeng Ji [a], Weishen Yang [a,*], Gongquan Sun [b], Qin Xin [a]

[a] State Key Laboratory of Catalysis, Dalian Institute of Chemical Physics, CAS, P.O. Box 110, Dalian 116023, China
[b] Direct Alcohol Fuel Cell Laboratory, Dalian Institute of Chemical Physics, CAS, P.O. Box 110, Dalian 116023, China

Abstract

In the present work, direct hydroxylation of benzene to phenol by using in situ generated H_2O_2 with electricity cogeneration was carried out in a *proton exchange membrane fuel cell* (PEMFC) reactor. Phenol was produced only when there was current through the external circuit. No other organic products were detected during this electrochemical process. A *rotating ring-disc electrode* (RRDE) technique was used to quantitatively detect the intermediate H_2O_2 in an acid electrolyte solution at different potentials and temperatures. The RRDE studies showed that the in situ generated H_2O_2 may play a crucial role during the formation of phenol. The formation rate of phenol could be controlled by adjusting the current or cell potential.

Keywords: Phenol; Oxidation; Membrane reactor; PEMFC; Electrochemical

1. Introduction

Phenol is a valuable chemical as an intermediate for the synthesis of various petrochemicals. Industrially, phenol has been mainly produced from benzene via the so-called "Cumene Process" which comprises three steps: (1) benzene alkylation to cumene, (2) cumene oxidation to cumene hydroperoxide, and (3) cumene hydroperoxide decomposition to phenol and acetone [1]. This three-step process suffers from not only the low overall yield (<5%) but also highly energy consuming. Furthermore, the market of the inevitable co-productive acetone is getting smaller and smaller than that of phenol. These reasons are the driving forces to approach a one-step synthesis of phenol. One of the routes reported is the gas-phase oxidation of benzene with N_2O over zeolite catalysts [1,2]. Another one is the direct liquid-phase hydroxylation of benzene with H_2O_2 [3]. But both oxidizing agents, N_2O and H_2O_2, are expensive. Oxygen is an ideal oxidant from environmental and economical points of view. However, the direct hydroxylation of benzene using oxygen and hydrogen is an unsafe and difficult reaction. Oxygen and hydrogen can be supplied separately using a membrane reactor, thus the danger of explosion can be avoided. Niwa et al. [4] reported an efficient one-step oxidation of benzene to phenol using a palladium membrane reactor.

Fuel cell, another kind of membrane reactor, is an electrochemical energy converter in which the free energy of a chemical reaction is directly converted into electricity. In the case of H_2–O_2 fuel cells, the electrochemical reaction at the anode and the cathode are hydrogen electro-oxidation and oxygen electro-reduction, respectively. Otsuka et al. first reported the one-step oxidation of benzene to phenol by using H_2–O_2 fuel cells both in liquid-phase [5] and gas-phase [6]. It is expected that the electrochemical reduction of oxygen on the proper electrocatalyst will generate active intermediate oxygen species. The essence of this process is the electrochemical generation of H_2O_2 on a cathode from oxygen and subsequent chemical reactions between its intermediates and an organic substrate [7].

The electrochemical *oxygen reduction reaction* (ORR) can proceed through two overall pathways, i.e. direct four-

---

* Corresponding author. Tel.: +86 411 84379073; fax: +86 411 84694447.
E-mail address: yangws@dicp.ac.cn (W. Yang).
URL: http://yanggroup.dicp.ac.cn

0920-5861/$ – see front matter © 2005 Elsevier B.V. All rights reserved.
doi:10.1016/j.cattod.2005.03.052

electron pathway and peroxide pathway which is mainly determined by the catalysts and the electrode potential [8]. Both pathways in acid electrolyte are shown below:

(1) Direct four-electron pathway:

$$O_2 + 4H^+ + 4e^- \rightarrow 2H_2O \qquad (1)$$

(2) Peroxide pathway:

$$O_2 + 2H^+ + 2e^- \rightarrow H_2O_2 \qquad (2)$$

followed by

$$H_2O_2 + 2H^+ + 2e^- \rightarrow 2H_2O_2 \qquad (3)$$

In the present investigation, we will report a controllable direct hydroxylation of benzene to phenol in a H_2–O_2 *proton exchange membrane fuel cell* (PEMFC) under usual fuel cell operation conditions. The in situ generated peroxide directly reacts with benzene to produce phenol. The process was proposed and presented in Fig. 1.

In order to know if the generation of H_2O_2 plays an important role during the phenol formation, *a rotating ring-disc electrode* (RRDE) technique was used to quantitatively detect the intermediate H_2O_2 in an acid electrolyte solution at different potentials and temperatures. The data obtained indicates this is indeed the case.

2. Experimental

In this work, a PEMFC using Nafion®-115 membrane as the electrolyte was adopted as a membrane reactor to produce phenol from benzene. The homemade Pd black and the commercial Pt black (Johnson Matthey Corp.) were used as oxygen-reduction and hydrogen-oxidation catalysts, respectively. Pd black was prepared by an impregnation–reduction method with formaldehyde as a reductive agent. Membrane electrode assembly (MEA) was fabricated by a modified decal transfer method, which has been described elsewhere in details [9]. The metal black loadings of both sides were 1.0 mg/cm². The electrode area was 9 cm².

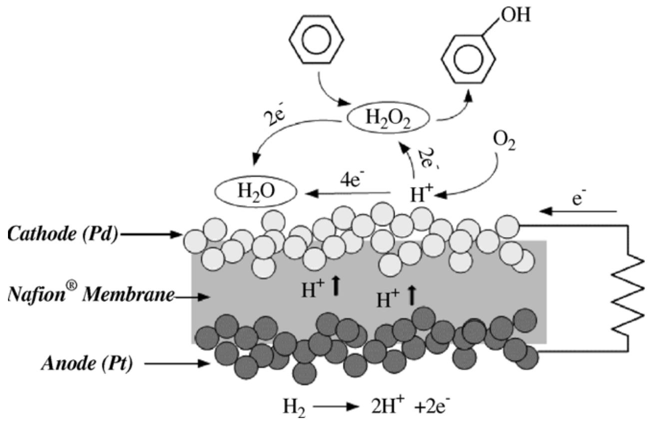

Fig. 1. Reaction scheme for the phenol synthesis using in situ generated H_2O_2 in a PEMFC reactor.

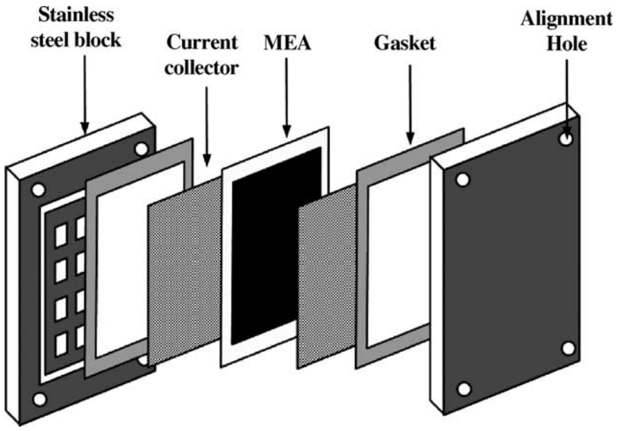

Fig. 2. Scheme of PEMFC reactor.

The PEMFC reactor was assembled as shown in Fig. 2. The MEA was sandwiched between two stainless steel blocks with dotted flow field. The insulation rubber gaskets were used to prevent the cell from leaking [10]. The whole apparatus used in this study is shown in Fig. 3. Benzene (73 μmol/min) was introduced by passing helium as carrier gas through a saturator in the constant temperature water bath (7 °C), and then mixed with oxygen at mole ratios of O_2:He:benzene = 30:13:1. The mixture was supplied to the cathode compartment at a pressure of 2 atm. Humidified hydrogen (1.7 mmol/min) was fed to the anode compartment at the same pressure as that of the cathode compartment. Current–voltage (*I*–*V*) data was obtained on a potentiostat/galvanostat (EG&G 263A) with the anode shorted to the reference electrode input. Cathode products were quantitatively analyzed by an online TCD/FID gas chromatograph (Agilent 6890) equipped with a HP-5 capillary column and a Porapak Q packed column.

RRDE technology is commonly used for studying the mechanism and detecting the intermediate of an electrochemical reaction, i.e. ORR [11,12]. If the ORR takes place on the disc electrode, the produced H_2O_2 will be oxidized on the ring electrode when the potential of this electrode is positive enough. The measurements were conducted in a glass cell with a GC/Pt RRDE electrode (Jiangfen, China) in 0.1 mol/L H_2SO_4 aqueous solution using a Pt electrode and a *saturated calomel electrode* (SCE) as the counter and reference electrodes, respectively. The well-dispersed ink with Pd black, Nafion® solution and water were quantitatively spread onto the surface of the glassy carbon disc electrode using a microsyringe. The electrolyte was saturated with oxygen for 15 min before the electrochemical measurement. The ring current is related to the disk current by the collection efficiency N because only part of the intermediate can be detected by the ring electrode. The theoretic collection efficiency, N_{th}, can be calculated with the geometric parameters (disc radius: 3.68 mm, ring inner radius: 4.44 mm, ring outer radius: 6.30 mm, $N_{th} = 0.551$

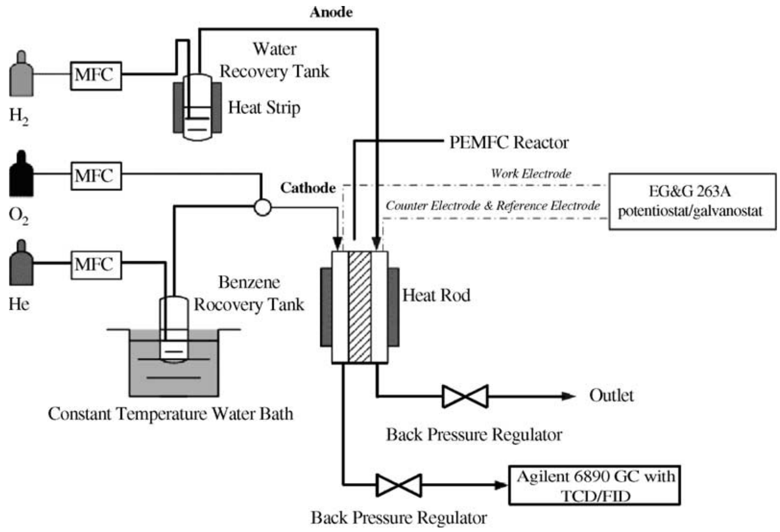

Fig. 3. Schematic configuration of the experimental apparatus.

[13]). The experimental collection efficiency of this RRDE was 0.556, which was measured using a solution of $K_3Fe(CN)_6$. Disc and ring potentials were controlled by a bi-potentiostat (Chenhua, China). The disc electrode potential was scanned from 0.8 V versus RHE to 0 V versus RHE at a scan rate of $10\,mV\,s^{-1}$. The Pt ring electrode was potentiostated at 1.2 V versus RHE in order to obtain the oxidation limiting current of H_2O_2 into oxygen. The rotation rate was set as 2400 rpm. All potentials in this study refer to that of the *reversible hydrogen electrode* (RHE).

3. Results and discussion

The polarization curves of PEMFC were obtained by adjusting the electronic resistance of the external load manually at different pressures at 60 and 90 °C (Fig. 4). It is a typical fuel cell process with benzene added to the cathodic compartment. The cell performance goes up along with not only the pressures but also the temperatures. Fig. 4 indicates that this process can be considered a kind of cogeneration process with high value products and electricity if phenol can be produced.

Under the experimental conditions mentioned above in PEMFC reactor, except unreacted benzene and phenol, no other organic compounds were detected from outlet of the cathode, which was different from the results that hydroquinone was also detected in literature [6]. Fig. 5 shows the effect of the current on the formation rate of phenol and the corresponding *I–V* data of PEMFC. The performance of PEMFC at 80 °C is much better than that at 60 °C. It also can be clearly seen from Fig. 5 that there is no phenol formation if the external circuit is open (there is no current through the external circuit). However, it is interesting to note that phenol can be detected if the external circuit is closed (current passes through the circuit). The phenol formation rates increase to the maximum values (0.17 μmol/min at 600 mA at 60 °C and 0.25 μmol/min at 900 mA at 80 °C), and then decrease with the current increase at both temperatures. From electrochemical point of view, the current, as a kinetic parameter, represents the reaction rate of the electrochemical reaction. Meanwhile, the

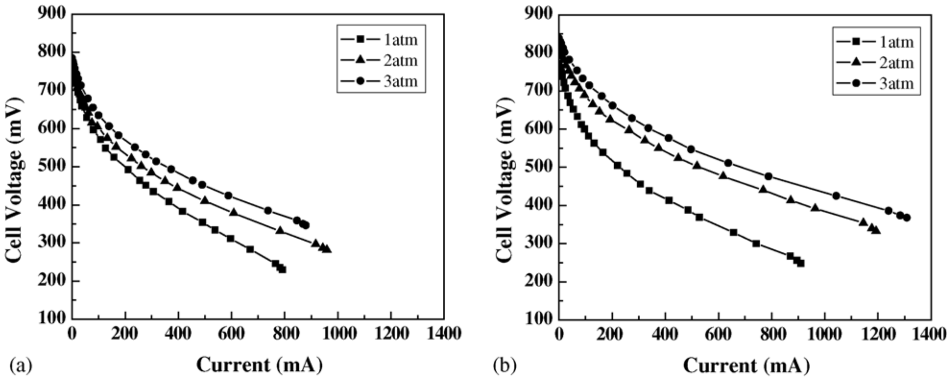

Fig. 4. Polarization curves of PEMFC with different pressures at 60 °C (a) and 90 °C (b). Anode: Pt black, 1.0 mg/cm^2, H_2, 2.2 mmol/min; cathode: Pd black, 1.0 mg/cm^2, water recovery tank, 5 °C higher than the reactor temperature, O_2, 2.2 mmol/min, He, 0.22 mmol/min, benzene recovery tank, 7 °C; electrolyte: Nafion®-115 membrane.

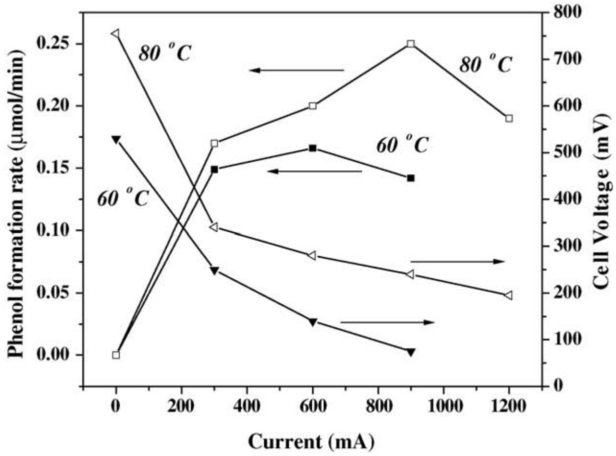

Fig. 5. Effects of current on the formation rate of phenol and the corresponding IV data of PEMFC at different temperatures. Anode: Pt black, 1.0 mg/cm^2, H_2 flow rate: 1.7 mmol/min, 2 atm; cathode: Pd black, 1.0 mg/cm^2, benzene flow rate: 73 μmol/min, O_2:He:benzene = 30:13:1, 2 atm; electrolyte: Nafion®-115 membrane.

voltage, as a thermodynamic parameter, controls what kind of reaction occurs. Taking the formation of in situ H_2O_2 into account, the observed volcano behavior of phenol formation is supposed to be closely related with the in situ H_2O_2 generation. At higher potential, oxygen reduction mainly proceeds through peroxide pathway, the amount of in situ generated H_2O_2 increases as the current increase, leading consequently to the improved phenol formation rate. On the other hand, in the lower potential range, the four-electron transfer process is predominant in the reaction of oxygen electro-reduction, which results in the decrease of the in situ generated H_2O_2. As a result, the formation rate of phenol decreases.

In order to know if there is any and how much peroxide intermediate H_2O_2 generated during the reaction in PEMFC reactor, RRDE technique was applied to quantitatively detect intermediate H_2O_2 generated in an acid electrolyte solution at different potentials and temperatures. In order to simulate H_2O_2 generation in PEMFC reactor, the Pd black catalyst spread on the disc electrode was same as the cathodic catalyst we used in the PEMFC reactor.

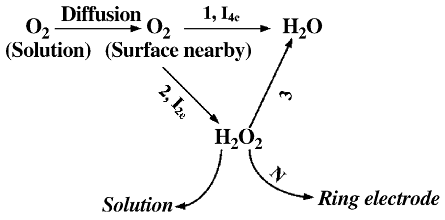

Fig. 7. A simple model for ORR.

The RRDE measurement process is shown in Fig. 6. A model for ORR shown in Fig. 7 was used to analyze the results in the present study which was first proposed by Damjanovic et al. [14]. The disk current (I_d) is the total reductive current of oxygen reduction including the two-electron (Eq. (2)) disc current (I_{2e}) and the four-electron (Eq. (1)) disc current (I_{4e}). The current related to Eq. (3) is included in I_{4e}.

$$I_d = I_{2e} + I_{4e} \tag{4}$$

Only part of the intermediate H_2O_2 can be captured by the ring electrode and oxidized to O_2. Therefore, the ring current (I_r) is

$$I_r = I_{2e} \times N \tag{5}$$

n_e is defined as the average number of exchanged electrons during the ORR of one molecular of oxygen. Thus,

$$\frac{I_d}{n_e} = \frac{I_{4e}}{4} + \frac{I_{2e}}{2} \tag{6}$$

n_e can be calculated from Eqs. (4)–(6) as,

$$n_e = \left[\frac{4I_d}{I_d + I_r/N}\right] \tag{7}$$

Then, the H_2O_2 molar proportion is

$$H_2O_2\,(\%) = \frac{I_{2e}/2}{I_d/n_e} \times 100\% = \frac{4 - n_e}{2} \times 100\% \tag{8}$$

Therefore, we can calculate the H_2O_2 molar proportion at different disc potentials and temperatures from RRDE experiment.

Fig. 8 shows the effects of the disc electrode potential on the currents of disk electrode (Fig. 8a) and ring electrode (Fig. 8b). Disk current increases when the disc electrode potential decreases (Fig. 8a), which may be caused by that more oxygen was involved in the ORR reaction or more oxygen was reduced via a complete four-electron pathway. The disk current at 80 °C is smaller than that at 60 °C, while

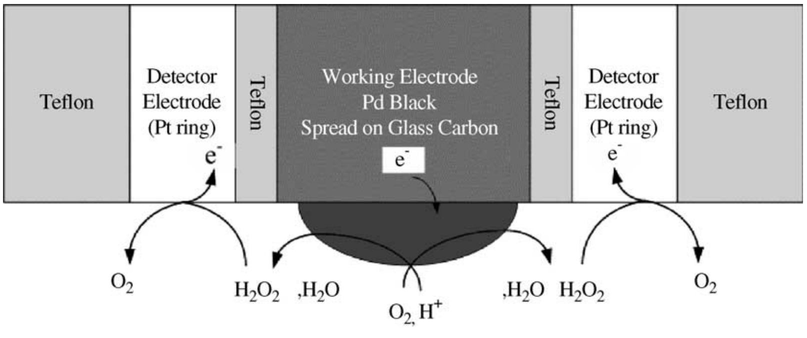

Fig. 6. RRDE measurement process for ORR.

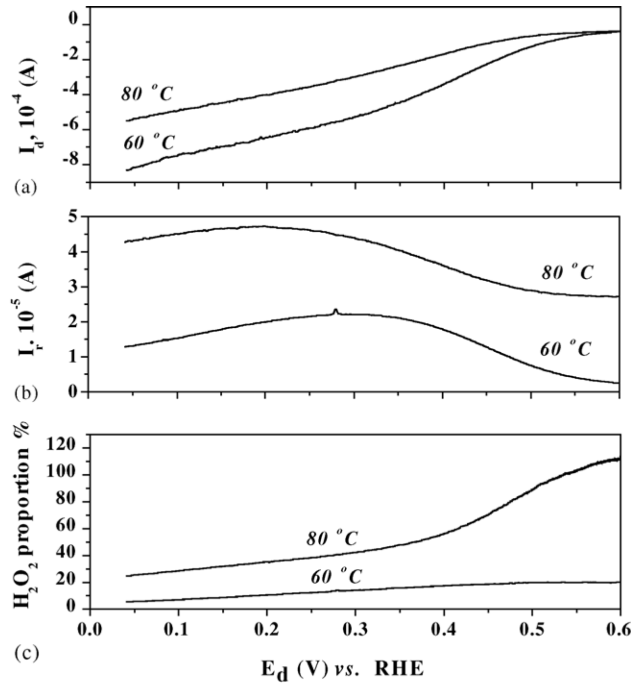

Fig. 8. (a) Oxygen reduction curves on the disk electrode; (b) H_2O_2 oxidation curves on the ring electrode; (c) H_2O_2 molar proportion. Pd black/GC disc electrode, Pt ring electrode in an oxygen saturated 0.1 mol/L H_2SO_4; scan rate of the disc potential, 10 mV s^{-1}; ring potential, 1.2 V; $N = 0.55$.

the ring current is contrary. This indicates that more oxygen was reduced through the four-electron pathway at 60 °C than 80 °C, but more H_2O_2 was produced on the ring electrode at 80 °C. From Fig. 8b, it can be found that the ring electrode currents increase with the reducing of disc electrode potential at first. Then, they reach their maximum and decrease. The phenomenon is similar to the behavior of the formation rate of phenol shown in Fig. 5. For the sake of explaining directly from the in situ generated H_2O_2, the molar proportion of H_2O_2 was calculated from I_d, I_r and N, shown in Fig. 8c. H_2O_2 molar proportion at 80 °C is much higher than that at 60 °C (about 100% near 0.6 V versus RHE at 80 °C) which indicates the reason why the formation rate of phenol is higher at 80 °C than that at 60 °C. It can also be seen that the proportion of H_2O_2 goes down along with the disc potential. Therefore the formation rate of H_2O_2 in our PEMFC reactor is controlled by the passing current and the cell voltage at the same time. The voltage always decreases with the current increase as a fuel cell system, which results in the appearance of the volcano behavior of the phenol formation rate in Fig. 5.

In order to explore the intrinsic catalytic activity of palladium black in the hydroxylation of benzene with hydrogen and oxygen, hydrogen was added to the cathode inlet gases. There is no phenol observed up to 80 °C. This means palladium black has no catalytic activity under such experimental conditions without current through the external circuit.

4. Conclusions

In conclusion, we have demonstrated a cogeneration process of electricity and the direct synthesis of phenol from benzene in a PEMFC reactor. This process can be well controlled by adjusting the current through the external circuit or the cell voltage. Further research is under investigation, such as: (1) screening more active or selective catalyst for improving PEMFC performance or enhancing oxygen reduction through the peroxide pathway; (2) modifying the cathodic catalyst for generating more active intermediate ($OH^{\bullet}$) to improve the oxidation efficiency of the phenol formation; (3) using other electrolyte membranes for higher temperature, such as, acid-doped polybenzimidazoles membrane and inorganic membranes.

Acknowledgements

The authors gratefully acknowledge financial supports from the National Nature Science of China (Grant No. 50332040) and the Ministry of Science and Technology, PR China (Grant No. G1999022401).

References

[1] G.I. Panov, A.S. Kharitonov, V.I. Sobolev, Appl. Catal. A: Gen. 98 (1993) 1.
[2] G.I. Panov, CATTECH 4 (2000) 18.
[3] L. Balducci, D. Bianchi, R. Bortolo, R. D'Aloisio, M. Ricci, R. Tassinari, R. Ungarelli, Angew. Chem. Int. Ed. 42 (2003) 4937.
[4] S. Niwa, M. Eswaramoorthy, J. Nair, A. Raj, N. Itoh, H. Shoji, T. Namba, F. Mizukami, Science 295 (2002) 105.
[5] K. Otsuka, K. Hosokawa, I. Yamanaka, Y. Wada, A. Morikawa, Electrochim. Acta 34 (1989) 1485–1488.
[6] I. Yamanaka, T. Akimoto, K. Otsuka, Electrochim. Acta 39 (1994) 2545–2549.
[7] V.L. Kornienko, G.A. Kolyagin, Russ. J. Electrochem. 39 (2003) 1308.
[8] L. Carrette, K.A. Friedrich, U. Stimming, CHEMPHYSCHEM 1 (2000) 162.
[9] S. Song, G. Wang, W. Zhou, X. Zhao, G. Sun, Q. Xin, S. Kontou, P. Tsiakaras, J. Power Sources 140 (2005) 103.
[10] Z.B. Wei, S.L. Wang, B.L. Yi, J.G. Liu, L.K. Chen, W.J. Zhou, W.Z. Li, Q. Xin, J. Power Sources 106 (2002) 364.
[11] O. Antoine, R. Durand, J. Appl. Electrochem. 30 (2000) 839.
[12] J. Maruyama, M. Inaba, Z. Ogumi, J. Electroanal. Chem. 458 (1998) 175.
[13] A.J. Bard, L.R. Faulkner, Electrochemical Methods: Fundamentals and Applications, 2nd ed. Wiley, New York, 2001, p. 351.
[14] A. Damjanovic, M.A. Genshaw, J.O.M. Bockris, J. Chem. Phys. 45 (1966) 4057.